Bending Rigidity of Interfaces in Aqueous Phase-Separated Biopolymer Mixtures

Elke Scholten, Leonard M. C. Sagis, and Erik van der Linden*

Physics Group, Department ATV, Wageningen University, Bomenweg 2, 6703 HD Wageningen, The Netherlands

Received: April 8, 2004; In Final Form: June 10, 2004

Using equations for the interfacial properties for a two-phase multicomponent system, we present a new model for the interfacial tension and bending rigidity for liquid−liquid interfaces between semidilute polymer phases. Using this model, we calculate the interfacial thickness and the bending rigidity for two different gelatin/dextran systems and a gelatin/gum arabic system using experimentally determined values for the interfacial tension. The bending rigidity of such systems has been unaccessible experimentally until now. For the gelatin/dextran systems, which are both near-critical, the interfacial thickness is very large (1000 nm) close to the critical point, where the interfacial tension is very low. Further from the critical point, the interfacial thickness decreases to a value in the order of the size of the biopolymers (100 nm). For the gelatin/gum arabic system, which is off-critical, we found the interfacial thickness to be constant, in the order of the size of the biopolymers. For the gelatin/dextran systems, the scaling relation between the interfacial tension and the interfacial thickness was investigated. The exponents were found to be approximately 1.7 for the two systems, which is in agreement with the exponent 2 of the scaling relation $\gamma \sim 1/\xi^2$. The accompanying bending rigidities for these near-critical gelatin/dextran systems were found to be approximately constant, with a value of 500 k_bT. The bending rigidity for the gelatin/gum arabic system, which is off-critical, was in the order of 25 k_bT. These high values for both the interfacial thickness and the bending rigidity for the near-critical systems may be of significance for interface-related phenomena in aqueous phase-separated biopolymer mixtures, in particular in cases where the bending contributions dominate the stretching contributions to the interfacial energy.

Introduction

When (bio)polymers are mixed at sufficiently high concentrations in water, phase separation may occur, and an interface will form between the two coexisting phases. The interfacial tension of phase-separated aqueous (bio)polymer systems is often very low, in the order of 1 μN/m.[1] In systems where the interfacial tension is small, the bending rigidity becomes important and may even dominate the behavior of the interface. Although the bending rigidity has been studied for vesicles and bilayers, for interfaces between aqueous phase-separated biopolymer systems this property has received little attention, nor has the interfacial thickness. Only for a colloid−polymer mixture have interfacial parameters been investigated. de Hoog and Lekkerkerker[2] reported interfacial tensions of a silica/poly(dimethylsiloxane) mixture, which are of the same order of magnitude as those of (bio)polymer mixtures. They also performed an ellipsometric study of the interface of this mixture, and from the results they found the interfacial thickness to be of the order of the size of the colloids.[3] Although these results are reasonable, they reported some experimental difficulties.[3] In general, measuring the ellipticity of phase-separated colloid−polymer or (bio)polymer systems is not easy. Since the interfacial tension is very low, the interfaces are very sensitive to small variations in temperature, mechanical vibrations, and fluctuations in pressure. Especially for samples that are close to the critical point, these variations can be of such significance that only a crude estimation of the order of magnitude for the interfacial thickness can be obtained. Although bending rigidities have been widely studied for microemulsion systems, for aqueous biopolymer interfaces, neither experimental data nor a theoretical model has been available. The experimental determination of rigidities for these mixtures following methods successful in microemulsions (i.e., light scattering or ellipsometry) has been unsuccessful until now since it is hampered by the fact that there is a small optical contrast between the two phases.

The main objective of this paper was to determine the bending rigidity and interfacial thickness for various aqueous phase-separated biopolymer systems, using experimental values of the (more easily accessible) interfacial tension as the only input variable. The procedure described circumvents the unresolved experimental difficulties of determining the bending rigidities and instead relies on using a combination of theory and experimental determination of the interfacial tension.

Theory

In the past decade, a large number of theories regarding interfacial properties have been published.[4−13] Here we will use the van der Waals theory, which introduces an intrinsic density profile across the interface that interpolates between the densities of the bulk phase. The usual approach in the van der Waals theory is to expand the free energy of the interface in terms of its curvature. From this expansion, we find that the surface tension up to the second order in curvature is given by[14]:

$$\gamma(J,K) = \gamma - kC_0J + \frac{1}{2}kJ^2 + \bar{k}K \qquad (1)$$

* Corresponding author e-mail: erik.vanderlinden@wur.nl.

10.1021/jp048439r CCC: $27.50
Published on Web 07/20/2004

where γ is the interfacial tension of the flat interface, k is the bending rigidity, C_0 is the spontaneous curvature of the interface, and $\bar{k}$ is the rigidity constant associated with the Gaussian curvature. J and K are the total curvature and Gaussian curvature, respectively. The first term signifies the stretching contribution to the interfacial energy, while the other terms relate to the bending contribution. The validity of this expression is limited to small curvature (i.e., for radii of curvature larger than the important length scales or interfacial thickness). Investigating the change in grand potential under local deformations for spherical and cylindrical cones, the following equations for γ and k for a two-component system have been obtained[8,13]:

$$\gamma = \frac{1}{4}\sum_{\alpha,\beta}\int \mathrm{d}z_1 \int \mathrm{d}r_{12} u'_{\alpha\beta}(r) r (1 - 3s^2)\rho_0^{\alpha\beta} \tag{2}$$

$$k = -\frac{1}{4}\sum_{\alpha,\beta}\int \mathrm{d}z_1 \int \mathrm{d}r_{12} u'_{\alpha\beta}(r) r \left[\frac{1}{2} z_1 z_2 (1 - 3s^2)\rho_0^{\alpha\beta} + \frac{1}{16} r^2 (1 + 6s^2 - 15s^4)\rho_0^{\alpha\beta} + (z_1 + z_2)(s^2 - \sin^2\phi_{12}(1 - s^2))\rho_{1c}^{\alpha\beta}\right] \tag{3}$$

where $u'_{\alpha\beta}$ is the derivative of the interaction potential between component α and β. Equation 3 is known as the Kirkwood−Buff formula,[15] and Groenewold and Bedeaux[13] extended this theory to obtain the result for γ and k for a multicomponent system. ρ_0 and ρ_{1c} refer to the first and second terms in the expansion of the pair density of a cylindrical interface. If we assume that $\rho_{c1}^{\alpha\beta}$ is independent of ϕ_{12}, eq 3 can be rewritten in the following form:

$$k = \frac{1}{8}\sum_{\alpha,\beta}\int \mathrm{d}z_1 \int \mathrm{d}r_{12} u'_{\alpha\beta}(r) r \left[(1 - 3s^2) z_1^{\,2} - \frac{1}{8} r^2 (1 + 6s^2 - 15s^4)\right]\rho_0^{\alpha\beta}(z_1, z_2, r) \tag{4}$$

To use eqs 2 and 4 for the calculation of γ and k, we need to assume a model for the pair density of the flat interface ($\rho_0^{\alpha\beta}$) and the pair potential ($u_{\alpha\beta}(r)$). For the pair density of a flat interface, we use the following approximate form:

$$\rho_0^{\alpha\beta}(z_1, z_2, r) = \rho^{\alpha}(z_1)\rho^{\beta}(z_2) g(r) \tag{5}$$

where $g(r)$ is the pair correlation function in a uniform liquid, and $\rho^{\alpha}(z_1)$ and $\rho^{\beta}(z_2)$ are the density profiles in the interfacial region. For the density profile, we assume the classical van der Waals profile:

$$\rho^{\alpha}(z) = \rho_c^{\alpha} - \frac{1}{2}\Delta\rho^{\alpha} \tanh(z/2\xi) \tag{6}$$

where ρ_c^{α} is the average of the densities of component α in the two bulk phases, $\Delta\rho^{\alpha} \equiv (\rho^{\alpha}_{\text{upperphase}} - \rho^{\alpha}_{\text{lowerphase}})$, and ξ is the interfacial thickness. Inserting eqs 5 and 6 in eqs 2 and 4 and integrating over z_1 gives

$$\gamma = \frac{1}{4}\pi\sum_{\alpha,\beta}\int_{-1}^{1} \mathrm{d}s \int_0^{\infty} \mathrm{d}r r^4 g(r) u'_{\alpha\beta}(r)(3s^3 - s) \operatorname{cotanh}(sr/2\xi)\Delta\rho^{\alpha}\Delta\rho^{\beta} \tag{7}$$

$$k = \frac{1}{24}\pi\sum_{\alpha,\beta}\int_{-1}^{1} \mathrm{d}s \int_0^{\infty} \mathrm{d}r r^4 g(r) u'_{\alpha\beta}(r)\left(\pi^2\xi^2(3s^3 - s) + \frac{1}{8} r^2 s(3 + 10s^2 - 21s^4)\right) \operatorname{cotanh}(sr/2\xi)\Delta\rho^{\alpha}\Delta\rho^{\beta} \tag{8}$$

For a single component ($\alpha = \beta = 1$), these equations reduce to the expressions for γ and k derived by Blokhuis and Bedeaux.[8] In the case of a two-component aqueous phase-separated system, α and β can both be either 1 or 2, which leads to four terms that contribute to the value of k.

For the interaction potential in eqs 7 and 8, we take a potential that has been derived from smoothed density theory,[16] where the distribution function of the distance of a segment from the center of mass of a molecule is used to derive the following equation:

$$\frac{u_{12}(r)}{k_b T} = \nu \int \rho_1(R)\rho_2(R - r)\, \mathrm{d}R \tag{9}$$

in which ν represents the excluded volume of a single monomer and $\rho_i(R)$ is the average segment density at distance R from the center of mass of isolated unperturbed chain i. The integral may be regarded as the effective volume excluded to one molecule by the presence of another. The segment densities $\rho_1(R)$ for the case of random chains are assumed to be Gaussian[16]:

$$\rho_i(r) = N_i\left(\frac{3}{2\pi R_{gi}^{\,2}}\right)^{3/2} \exp\left(-\frac{3r_i^{\,2}}{2R_{gi}^{\,2}}\right) \tag{10}$$

where N_i is the total amount of monomers, R_{gi} represents the radius of gyration of the polymers, and r_i is the distance of the volume element from the respective center of gravity. Substituting the Gaussian distribution (eq 10) in the expression for the interaction potential (eq 9) gives the interaction potential for a system with two polymers, with radius of gyration $R_{g,i}$:

$$u_{12}(r) = k_b T \nu N_1 N_2 \left(\frac{1}{2\pi}\right)^{3/2}\left(\frac{3}{(R_{g,1}^{\,2} + R_{g,2}^{\,2})}\right)^{3/2} \exp\left(\frac{-3r^2}{2(R_{g,1}^{\,2} + R_{g,2}^{\,2})}\right) \tag{11}$$

In this equation k_b is the Boltzmann constant, T is the temperature, ν is the excluded volume of a monomer and N_i is the amount of monomers of biopolymer 1 or 2, respectively. This interaction potential is also known as the Flory−Krigbaum potential,[17] which was derived for a dilute solution of heterogeneous polymers in 1950.

We used this model to predict the interfacial thickness and the bending rigidity for phase-separated protein/polysaccharide mixtures. Phase separation in such mixtures results in an upper phase enriched in protein and a lower phase concentrated in polysaccharide. Due to the distribution of polymers, the protein concentration in the lower phase will be below the overlap concentration (c^*). In the upper phase, however, the concentration is above c^*, and the solution is in the semidilute regime. While being in the dilute regime in the upper phase, the polysaccharide is present in the semidilute regime in the lower phase. In a semidilute solution, a network with a certain blob size (ζ) is formed, which can be calculated using[18]

$$\zeta = R_g\left(\frac{c^*}{c}\right)^{3/4} \tag{12}$$

TABLE 1: Molecular Weight (M), Radius of Gyration (R_g), Monomer Weight of Biopolymers (M_{mon}), and Kuhn Length of Monomers (b)[1,20]

biopolymer	solvent	M (kg/mol)	R_g (nm)	M_{mon} (g/mol)	b (nm)
gelatin	1 M NaI, pH 6	41	6.7	100	0.81
	0.5 M NaI, pH 8.5	41	7.0		0.85
dextran A	1 M NaI, pH 6	387	17.5	180	0.92
dextran B	0.5 M NaI, pH 8,5	579	19.4	180	0.84
gum arabic	0.5 M NaI, pH 8.5	580	15.4	180	0.66

The overlap concentration (c^*) is given by

$$c^* = \frac{3M}{4\pi R_g^{\,3} N_{av}} \tag{13}$$

where M is the molecular weight of the polymer and N_{av} is Avogadro's number. For each polymer, two different length scales are important; the radius of gyration in the dilute phase and the blob size (ζ) in the semidilute phase. To simplify the integrations in eqs 7 and 8, we take the average length scale of both phases ($\tilde{\zeta}$) defined by

$$\tilde{\zeta} = \left(\frac{R_g + \zeta}{2}\right) \tag{14}$$

This can be considered an average blob size of the system. Inserting $\tilde{\zeta}$ into eq 11, the interaction potential for a two-component two-phase system becomes

$$u_{\alpha\beta}(r) = k_b T \nu N_{blob}^{\alpha} N_{blob}^{\beta} \left(\frac{1}{2\pi}\right)^{3/2} \left(\frac{3}{(\tilde{\zeta}_\alpha^{\,2} + \tilde{\zeta}_\beta^{\,2})}\right)^{3/2} \exp\left(\frac{-3r^2}{2(\tilde{\zeta}_\alpha^{\,2} + \tilde{\zeta}_\beta^{\,2})}\right) \tag{15}$$

For the excluded volume ν, we take the size of a cylinder $\nu = \pi b^3$, in which b is the Kuhn segment length. For b, we take the average Kuhn length of the biopolymers, which can be calculated from the radius of gyration, using $b = \sqrt{6R_g^{\,2}/N}$.[19] The number of monomers in a blob ($N_{blob}^{\alpha,\beta}$) is calculated using $N_{blob}^{\alpha,\beta} = 6\tilde{\zeta}_{,\alpha\beta}^{\,2}/b^2$.

Materials

To obtain phase-separated protein/polysaccharide mixtures, we used gelatin as a protein mixed with either dextran or gum arabic, which are both polysaccharides. Gelatin was mixed with dextran A in a 1 M NaI solution at pH 6. In a 0.5 M NaI solution at pH 8.5, gelatin was mixed with either dextran B or gum arabic. Sodium iodide was added to suppress the gelation of the gelatin. The alkaline environment was used to obtain a negatively charged gelatin (pI = ±5.5) to prevent complex coascervation of gelatin with negatively charged gum arabic. Table 1 gives an overview of the properties of these biopolymers in the different solutions.

The phase diagrams and the interfacial tension of these phase-separated protein/polysaccharide mixtures have been determined previously.[1,20] The interfacial tensions were measured using the spinning drop technique, in which deformation of a macroscopically large droplet (mm) is measured. The phase diagrams were constructed by determining the concentrations of the biopolymers in both phases using polarimetry. Using these concentrations and the properties of the biopolymers, we determined the different length scales of the biopolymers in both the upper and lower phase, and from these calculations we determined the average blob size ($\tilde{\zeta}$) and the number of monomers (N_{blob}). An overview can be found in Tables 2−4.

TABLE 2: Density Difference of Gelatin ($\Delta\rho_{gel}$), Density Difference of Dextran ($\Delta\rho_{dex}$), Average Blob Size of Gelatin ($\tilde{\zeta}_{gel}$), Average Blob Size of Dextran ($\tilde{\zeta}_{dex}$), Number of Gelatin Monomers in a Blob ($N_{blob,gel}$), and Number of Dextran Monomers in a Blob ($N_{blob,dex}$) for Gelatin/Dextran A System

$\Delta\rho_{gel}$ (molecules/m^3)	$\Delta\rho_{dex}$ (molecules/m^3)	$\tilde{\zeta}_{gel}$ (nm)	$\tilde{\zeta}_{dex}$ (nm)	$N_{blob,gel}$ (molecules)	$N_{blob,dex}$ (molecules)
6.31×10^{23}	-6.36×10^{22}	5.4	14.3	266	1449
1.14×10^{24}	-9.22×10^{22}	5.2	13.2	247	1235
1.52×10^{24}	-1.10×10^{23}	4.9	12.8	219	1161
2.47×10^{24}	-1.65×10^{23}	4.6	11.8	193	987
2.68×10^{24}	$-1{,}96 \times 10^{23}$	4.6	11.5	193	938

TABLE 3: Density Difference of Gelatin ($\Delta\rho_{gel}$), Density Difference of Dextran ($\Delta\rho_{dex}$), Average Blob Size of Gelatin ($\tilde{\zeta}_{gel}$), Average Blob Size of Dextran ($\tilde{\zeta}_{dex}$), Number of Gelatin Monomers in a Blob ($N_{blob,gel}$), and Number of Dextran Monomers in a Blob ($N_{blob,dex}$) for Gelatin/Dextran B System

$\Delta\rho_{gel}$ (molecules/m^3)	$\Delta\rho_{dex}$ (molecules/m^3)	$\tilde{\zeta}_{gel}$ (nm)	$\tilde{\zeta}_{dex}$ (nm)	$N_{blob,gel}$ (molecules)	$N_{blob,dex}$ (molecules)
8.86×10^{23}	-5.07×10^{22}	5.0	15.6	206	2056
1.33×10^{24}	-6.79×10^{22}	5.0	14.9	218	1888
1.56×10^{24}	-8.29×10^{22}	4.9	14.2	208	1710
1.95×10^{24}	-1.02×10^{23}	4.8	13.7	196	1603
2.09×10^{24}	-1.11×10^{23}	4.8	13.4	195	1529
2.42×10^{24}	$-1{,}22 \times 10^{23}$	4.7	13.2	187	1481

TABLE 4: Density Difference of Gelatin ($\Delta\rho_{gel}$), Density Difference of Gum Arabic ($\Delta\rho_{gum}$), Average Blob Size of Gelatin ($\tilde{\zeta}_{gel}$), Average Blob Size of Gum Arabic ($\tilde{\zeta}_{ara}$), Number of Gelatin Monomers in a Blob ($N_{blob,gel}$), and Number of Gum Arabic Monomers in a Blob ($N_{blob,ara}$) for Gelatin/Gum Arabic System

$\Delta\rho_{gel}$ (molecules/m^3)	$\Delta\rho_{ara}$ (molecules/m^3)	$\tilde{\zeta}_{gel}$ (nm)	$\tilde{\zeta}_{ara}$ (nm)	$N_{blob,gel}$ (molecules)	$N_{blob,ara}$ (molecules)
7.83×10^{23}	-4.54×10^{22}	5.6	15.3	265	3209
6.75×10^{23}	-5.41×10^{22}	5.7	14.0	279	2707
1.11×10^{24}	-8.93×10^{22}	5.4	13.1	244	2370
1.39×10^{24}	-1.20×10^{23}	5.2	12.3	228	2072
1.74×10^{24}	-1.50×10^{23}	5.0	11.6	214	1867

Results and Discussion

The values for the average blob size of the biopolymers, the amount of monomers present in this blob size, and the excluded volume were inserted into eq 15 to obtain the interaction potential for the different systems. Since the interfacial tension of these systems is known, we could substitute this value for the interaction potential into eq 7 and estimate the interfacial thickness. For the pair correlation function we assumed $g(r) = 1$, the correlation function for an ideal fluid. The values for the interfacial thickness were substituted in eq 8 to obtain the bending rigidity. The results of these calculations are presented in Tables 5 (gelatin/dextran A), 6 (gelatin/dextran B), and 7 (gelatin/gum arabic).

Interfacial Thickness and Scaling Behavior. The interfacial tension can be estimated from the scaling relation $\gamma \propto (kT/\xi^2)$.[18,21] To confirm whether this relation is observed for these different protein/polysaccharide systems, the interfacial tension is plotted against the interfacial thickness and fitted with $\gamma = a/\xi^b$.

Figure 1 shows this relation for both gelatin/dextran systems. For the gelatin/dextran A system (squares), $b = 1.7 \pm 0.1$ gave the best fit. For the gelatin/dextran B system (triangles), b was found to be 1.7 ± 0.2. The exponent b for both systems is in

TABLE 5: Interfacial Tension (γ), Interfacial Thickness (ξ), and Bending Rigidity (k) for Gelatin/Dextran A System

interfacial tension (μN/m)	interfacial thickness[a] (nm)	bending rigidity[a,b] (k_bT)
0.5 ± 0.1	956 ± 239	418 ± 98
2.4 ± 0.3	408 ± 58	369 ± 49
5.9 ± 0.5	214 ± 19	241 ± 22
15.7 ± 0.7	117 ± 5	192 ± 10
19.3 ± 0.8	108 ± 5	202 ± 10

[a] ξ and k are calculated according to the model. Only γ is measured experimentally.[1] [b] Temperature (T) is taken as 293 K.

TABLE 6: Interfacial Tension (γ), Interfacial Thickness (ξ), and Bending Rigidity (k) for Gelatin/Dextran B System

interfacial tension (μN/m)	interfacial thickness[a] (nm)	bending rigidity[a,b] (k_bT)
0.6 ± 0.1	1190 ± 610	763 ± 394
1.9 ± 0.3	760 ± 140	985 ± 175
3.4 ± 0.3	470 ± 45	665 ± 73
5.3 ± 0.4	386 ± 31	714 ± 49
7.1 ± 0.4	300 ± 18	566 ± 49
9.1 ± 0.6	273 ± 19	615 ± 49

[a] ξ and k are calculated according to the model. Only γ is measured experimentally.[20] [b] Temperature (T) is taken as 293 K.

TABLE 7: Interfacial Tension (γ), Interfacial Thickness (ξ), and Bending Rigidity (k) for Gelatin/Gum Arabic System

sample no.	interfacial tension (μN/m)	interfacial thickness[a] (nm)	bending rigidity[a,b] (k_bT)
C1	1.5 ± 0.2	362 ± 56	180 ± 28
C2	6.7 ± 1.2	43 ± 9	12 ± 3
C3	9.7 ± 1.5	52 ± 10	25 ± 5
C4	12.9 ± 1.9	47 ± 7	26 ± 4
C5	14.9 ± 2.4	53 ± 9	33 ± 6

[a] ξ and k are calculated according to the model. Only γ is measured experimentally.[20] [b] Temperature (T) is taken as 293 K.

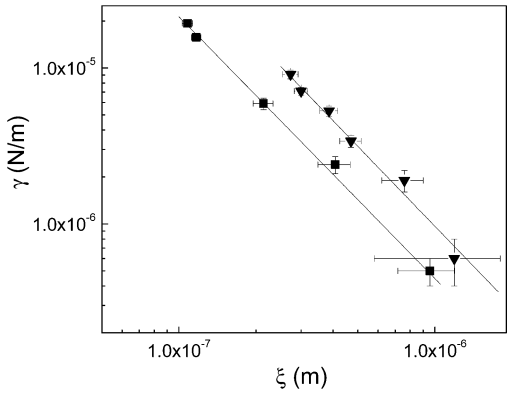

Figure 1. Interfacial tension γ vs interfacial thickness ξ for the gelatin/dextran A system (squares) and the gelatin/dextran B system (triangles).

line with a theoretically expected value of 2. The thickness of the interfacial region for both systems is very large close to the critical point where the interfacial tension is very low. Further from the critical point, where the interfacial tension increases, the interfacial thickness decreases to a value in the order of the size of the polymers (100 nm). The gelatin/gum arabic system, however, does not show this scaling relation. As can be seen in Figure 2, the thickness of the interfacial region is approximately constant within the statistical error and is found to be ± 50 nm, which is of the order of the size of the biopolymers. Only the interfacial thickness for sample C1 deviates from this value. Since this sample was close to the critical point, the compositions of this sample were difficult to determine, and as a result,

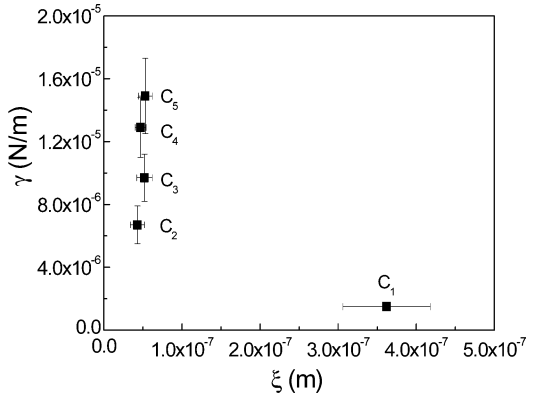

Figure 2. Interfacial tension γ vs interfacial thickness ξ for the gelatin/gum arabic system.

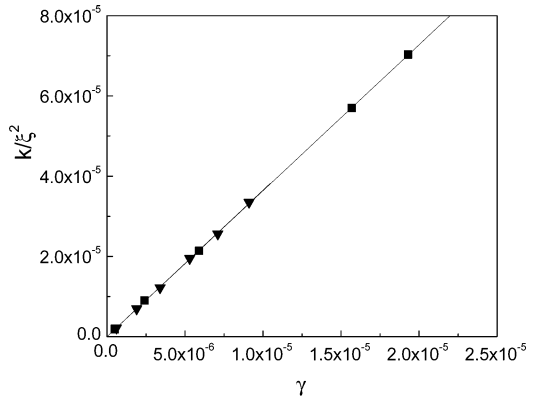

Figure 3. k/ξ^2 vs interfacial tension γ for the gelatin/dextran A system (squares) and the gelatin/dextran B system (triangles).

they do not coincide with the determined binodal.[20] These small deviations from the binodal have a great influence on the determination of the interfacial thickness.

From interfacial tension measurements and scaling behavior, we conclude that the gelatin/dextran systems are both near-critical and that the gelatin/gum arabic system was off-critical in the investigated concentration regime.[1,20] Since the interfacial thickness in the critical point diverges, this indicates that mixtures that are near-critical should have diffuse interfacial regions that increase as the critical point is approached. For the gelatin/dextran systems this is indeed the case and can thus be considered to be near-critical. Going further from the critical point, the interfacial layer decreases and the system becomes off-critical. Since the gelatin/gum arabic has a constant value for the interfacial thickness for all investigated samples, this system can be considered to be off-critical.

Bending Rigidity and Scaling Behavior. In Tables 5 and 6, we see that the bending rigidity is approximately constant within the statistical errors for the near-critical gelatin/dextran systems and is of the order of $200-1000\ k_bT$. For the off-critical gelatin/gum arabic system (Table 7), the bending rigidity is approximately $25\ k_bT$. Because of the uncertainty in the interfacial thickness for sample C1, we attach little importance to the value of the bending rigidity of this particular sample.

According to Blokhuis and Bedeaux.[8] the bending rigidity close to the critical point, where $\xi \rightarrow \infty$, is given by

$$k = \left(\frac{1}{6}\pi^2 + 2\right)\gamma\xi^2 = 3.64\gamma\xi^2 \qquad (16)$$

Since both the gelatin/dextran systems are near-critical, these systems should obey this relation. As can be seen in Figure 3,

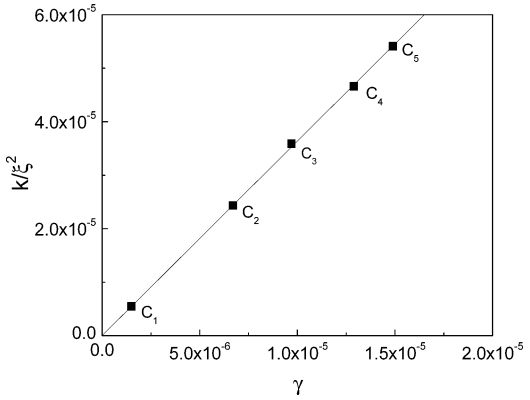

Figure 4. k/ξ^2 vs interfacial tension γ for the gelatin/gum arabic system.

this linear relationship is indeed obtained for both systems, with a slope of 3.65, in correspondence with the pre-factor in eq 16. For off-critical systems ($\xi \rightarrow 0$), Blokhuis and Bedeaux did not find such a relationship. However, when we plot k/ξ^2 versus γ for the off-critical gelatin/gum arabic system, we again observe a linear relationship (Figure 4) for which the slope again corresponds with the pre-factor, 3.64, of eq 16. This linear relationship holds for all investigated protein/polysaccharide systems, and the bending rigidity can thus be determined for both near-critical and off-critical systems according to eq 16.

Since this equation is satisfied for all our investigated systems, we can simply invert it to find $\gamma = k/3.64\xi^2$. We see that in the near-critical gelatin/dextran systems, in which the relation $\gamma \sim 1/\xi^2$ holds, k is a constant that can be determined from the slope of γ versus $1/\xi^2$. Using this relation for the near-critical systems, the bending rigidity was determined to be 200 k_bT for the gelatin/dextran A system and 615 k_bT for the gelatin/dextran B system. Contradictory to the near-critical samples, the off-critical gelatin/gum arabic system shows a constant interfacial thickness for the investigated concentration regime. Since eq 16 is also satisfied for this system, the bending rigidity is not expected to be constant but should increase with increasing interfacial tension (as the interfacial thickness is constant). Analogous to the procedure of calculating the bending rigidity from the interfacial thickness in near-critical systems, we can determine the interfacial thickness from the bending rigidity in off-critical systems. The relation $k = 3.64\gamma\xi^2$ shows that plotting the bending rigidity (k) versus the interfacial tension (γ) gives the interfacial thickness from the slope. Using this relation for the gelatin/gum arabic system, we obtain an interfacial thickness of 50 nm.

Thus, even though for all systems the interfacial tension increases as the distance from the critical point increases, we find different scaling for the two other interfacial properties. In the case of near-critical systems, we find a decreasing interfacial thickness with increasing distance from the critical point and a constant bending rigidity. In the case of off-critical systems, we find a constant interfacial thickness, and the bending rigidity increases slightly with increasing distance from the critical point.

The bending rigidities of the investigated off-critical gelatin/gum arabic system are comparable to those found in microemulsions and vesicle systems. However, the bending rigidities of the near-critical gelatin/dextran systems are much larger. Although the bending rigidities of vesicles and bilayers are normally of the order of 10 k_bT, Bermudez et al.[22] recently reported for vesicles formed from OB18 ($PEO_{80}-PBD_{125}$), with a membrane thickness of 14.8 nm, bending rigidities of 460 k_bT, which are comparable to the values we found for the near-critical systems. Since the interfacial tension of these systems is very low, the bending contribution to the interfacial energy may become dominant over the stretching contribution for several interfacial-related phenomena. For instance, relaxation times in bending-dominated systems will exhibit a different scaling with the droplet radius (R) compared to when the stretching contribution would be dominant (difference of a factor R^2). This may for instance apply to situations where deformation relaxation of a droplet interface occurs upon change in volume, while maintaining a constant area (thus making the stretching contribution irrelevant). Such a droplet deformation may in particular apply to aqueous phase-separated systems, where water exchange between the bulk phases is possible. Another situation where bending may dominate over stretching may occur at a droplet size where the bending energy, which is independent of the surface area, becomes larger than the stretching energy, which is dependent on the surface area of a droplet. Thus, there exists a particular crossover length scale (R_c) below which bending dominates over stretching. A rough estimate of this crossover length scale can be given by considering the two contributions to the interfacial energy to be equal. The interfacial free energy can be given as an integral over the surface as

$$F = \int\left(\gamma + \frac{2k}{R^2}\right) \mathrm{d}A \tag{17}$$

in which the first term signifies the stretching term, and the second term signifies the bending term. Integrating over the surface yields for the stretching term $4\pi\gamma R^2$ and for the bending term $8\pi k$. Equating these two terms gives $\sqrt{R_c=2k/\gamma}$, the critical radius below which bending dominates stretching. Using $\gamma \sim O(10^{-6})$ N/m and $k \sim O(100)$ k_bT, we find $R_c \sim O(1000)$ nm. Since the interfacial tension can also be given in terms of the bending rigidity, $\gamma = k/3.64\xi^2$, we find that $R_c = 2.7\xi$ (i.e., thus the critical radius is of the same order of magnitude as the interfacial thickness). We stress that, since R_c becomes comparable to the interfacial thickness in these systems, the curvature cannot be considered to be small and eqs 1 and 6 might not be valid in this limit. In this limit one has to take into account higher order terms in curvature and density profile. Thus, R_c can be considered as a rough estimate only. Using this estimation we find that for droplet radii smaller than 1 μm the contribution of the bending energy is expected to become important for these systems. This length scale is relevant to many practical circumstances (e.g., to shear-induced phase separation and shear-induced droplet morphologies). It is also expected to be of relevance to the kinetics of phase separation in aqueous biopolymer systems, during stages where the domain size is smaller than R_c.

Conclusion

In this paper we present a new model to calculate the interfacial thickness and bending rigidity for aqueous phase-separated biopolymer mixtures on the basis of the experimentally accessible interfacial tension. We determined these interfacial properties for three different protein/polysaccharide systems: two gelatin/dextran systems and one gelatin/gum arabic system. For the gelatin/dextran systems, the interfacial thickness was large for samples close to the critical point (1000 nm) and decreased for samples further from the critical point. The presence of the diffuse interfacial region indicated that the systems could be considered to be near-critical. For the gelatin/gum arabic system, the interfacial region was found to be constant and of the order of the size of the biopolymers (50

nm), which indicates that this system is off-critical. Using the calculated interfacial thickness, we determined the bending rigidities of the systems. For the gelatin/dextran systems, the bending rigidity was found to be in the order of 500 k_bT; for the gelatin/gum arabic system, we found values of approximately 25 k_bT. The values for the interfacial thickness and the bending rigidity of the near-critical systems are much higher than those found in microemulsion systems and may be important when the bending contribution to the interfacial energy dominates the stretching contribution. This might be of relevance in several interfacial phenomena, such as droplet relaxation, shear-induced phase separation, and shear-induced droplet morphologies.

Acknowledgment. We thank E. Blokhuis and H. Schaink for stimulating and helpful discussions.

References and Notes

(1) Scholten, E.; Tuinier, R.; Tromp, R. H.; Lekkerkerker, H. N. W. *Langmuir* **2002**, *18*, 2234−2238.
(2) de Hoog, E. H. A.; Lekkerkerker, H. N. W. *J. Phys. Chem.* **1999**, *103*, 5274−5279.
(3) de Hoog, E. H. A.; Lekkerkerker, H. N. W.; Schulz, J.; Findenegg, G. H. *J. Phys. Chem.* **1999**, *103*, 10657−10660.
(4) Milchev, A.; Binder, K. *Europhys. Lett.* **2002**, *59*, 81−86.
(5) Mecke, K. R.; Dietrich, S. *Phys. Rev. E* **1999**, *59*, 6766−6784.
(6) Blokhuis, E. M.; Bedeaux, D. *HCR Adv. Educ. Rev.* **1994**, 55−68.
(7) Blokhuis, E. M.; Bedeaux, D. *J. Chem. Phys.* **1991**, *95*, 6986−6988.
(8) Blokhuis, E. M.; Bedeaux, D. *Physica A* **1992**, *184*, 42−70.
(9) van Giessen, A. E.; Blokhuis, E. M. *J. Chem. Phys.* **2002**, *116*, 302−310.
(10) Oversteegen, S. M.; Blokhuis, E. M. *J. Chem. Phys.* **2000**, *112*, 2980−2986.
(11) Segovia-Lopez, J. G.; Romero-Rochin, V. *Phys. Rev. Lett.* **2001**, *86*, 2369−2372.
(12) Varea, C.; Robledo, A. *Physica A* **1995**, *220*, 33−47.
(13) Groenewold, J.; Bedeaux, D. *Physica A* **1995**, *214*, 356−378.
(14) Helfrich, W. *Z. Naturforsch.* **1973**, *28c*, 693.
(15) Kirkwood, J. G.; Buff, F. P. *J. Chem. Phys.* **1949**, *17*, 338−343.
(16) Yamakawa, H. *Modern Theory of Polymer Solutions*; Harper & Row: New York, 1971.
(17) Flory, P. J.; Krigbaum, W. R. *J. Chem. Phys.* **1950**, *18*, 1086−1094.
(18) de Gennes, P. G. *Scaling Concepts in Polymer Physics*; Cornell University Press: New York, 1979.
(19) Doi, M.; Edwards, S. F. *The Theory of Polymer Dynamics*; Clarendon Press: Oxford, 1999.
(20) Scholten, E.; Visser, J. E.; Sagis, L. M. C.; van der Linden, E. *Langmuir* **2004**, *20*, 2292−2297.
(21) Rowlinson, J. S.; Widom, B. *Molecular Theory of Capillarity*; Clarendon Press: Oxford, 1984.
(22) Bermudez, H.; Hammer, D. A.; Discher, D. E. *Langmuir* **2004**, *20*, 540−543.